Bull. Soc. R. Sci. Liège, 2024, **93**(3), 363–373 *Peer-reviewed conference paper*
doi:10.25518/0037-9565.12414

Compact Objects with Wolf–Rayet Companions: a Key Binary Configuration to Produce Gravitational Wave Mergers

Erika KORB[1,2,3]

[1] Physics and Astronomy Department, University of Padova, Vicolo dell'Osservatorio 3, I–35122, Padova, Italy
[2] INFN – Padova, Via Marzolo 8, I–35131 Padova, Italy
[3] Institut für Theoretische Astrophysik, ZAH, Universität Heidelberg, Albert-Ueberle-Straße 2, D–69120 Heidelberg, Germany
Correspondence to: erika.korb@studenti.unipd.it

Paper presented at the 41st Liège International Astrophysical Colloquium on "The eventful life of massive star multiples," University of Liège (Belgium), 15–19 July 2024.

Abstract

The properties of binaries hosting a Wolf–Rayet star and a compact object (black hole or neutron star) suggest that such systems could be the progenitors of binary compact objects merging via gravitational wave emission. We used the population-synthesis code `SEVN` to explore this possibility and account for current uncertainties in theoretical models. According to our simulations, most (more than about 83%) binary compact object mergers were once compact objects with Wolf–Rayet companions. Binaries like Cyg X-3, the only candidate hosting a Wolf–Rayet and a compact object observed in the Milky Way, are more likely (approximately 70%–100%) to become binary compact object mergers if they host a black hole. This work indicates that further characterization of systems like Cyg X-3 can unveil the formation mechanisms of binary compact object mergers.

Keywords: Wolf–Rayet star, black hole, neutron star, gravitational waves, binary evolution, population-synthesis, Cyg X-3

1. Introduction

The gravitational wave detectors of the LIGO–Virgo–KAGRA collaboration observed so far about 100 binary compact object mergers (BCOs) candidate events (Abbott et al., 2023). The formation channels of BCOs are still unclear because crucial processes in binary evolution, such as mass-transfer and core-collapse supernovae (CCSNe), are still poorly understood (see the reviews by Mapelli (2021), Mandel and Broekgaarden (2022), and references therein). After a mass-transfer event, the external layers of the donor star can be completely removed and the star could be visible as a Wolf–Rayet (WR) one (e.g., Crowther, 2007; Bethe and Brown, 1998; Tauris et al., 2017; Kruckow et al., 2018). Thus, binaries hosting a WR star and a compact object

(WR–COs) have been proposed as possible progenitors of BCOs (Bulik et al., 2011; Belczynski et al., 2013; Schneider et al., 2023). If WR–COs were confirmed to be the progenitors of BCOs, we could exploit observations of WR–COs to constrain the interpretation of the evolutionary channels of BCOs.

2. A Population-synthesis Approach

We used the population-synthesis code `SEVN` (Iorio et al., 2023) to characterize the role played by WR–COs in the formation of BCOs. We accounted for model uncertainties by simulating the same initial population of binaries and changing the model assumptions. We simulated the evolution of a population of 5×10^6 binaries and sampled the initial masses of the primary star $M_1 \geq M_2$ from the Kroupa (2001) initial mass function ($\xi(M_1) \propto M_1^{-2.3}$, with $5 M_\odot \leq M_1 \leq 150 M_\odot$). Mass ratios $q = M_2/M_1$ and orbital periods $\mathscr{P} = \log(P/\text{days})$ were taken from Sana et al. (2012): $\xi(q) \propto q^{-0.1}$ for $0.1 \leq q \leq 1$, and $\xi(\mathscr{P}) \propto \mathscr{P}^{-0.55}$ for $0.30 \leq \mathscr{P} \leq 5.5$, respectively. The initial eccentricity distribution e accounts for the dependence on the orbital period P observed by Moe and Di Stefano (2017): $\xi(e(P)) \propto 1 - (P/\text{days})^{-2/3}$ for $P \geq 2$ days.

We considered the possibility that it may take less than 250 milliseconds or more than 250 milliseconds after the core bounce for the neutrino-driven explosion in CCSNe events to be revived—hereafter, rapid or delayed CCSNe models, respectively—as in Fryer et al. (2012). We also tested the CCSN model adopted by Mapelli et al. (2020), that is based on the compactness parameter of O'Connor and Ott (2011). This compactness-based CCSN model assumes that stars with a compact structure at the onset of the core-collapse will collapse into black holes (BHs) and will not successfully explode as supernovae, limiting neutron star (NS) formation.

CCSN explosions are not symmetric events: the new-born CO receives a natal kick as a result of asymmetric mass loss. Given the stochastic nature of the process, we extracted natal kick magnitudes from the velocity distribution of the COs observed in the Galaxy, testing various models to account for fallback and linear momentum conservation. In the first model (hereafter, M265 model) we draw natal kick magnitudes from a Maxwellian distribution with a root-mean-square speed $\sigma = 265\,\text{km}\,\text{s}^{-1}$, representative of the observed Galactic pulsar proper motions (Hobbs et al., 2005). Similarly, in the second model (M70), we draw the velocities from a Maxwellian with $\sigma = 70\,\text{km}\,\text{s}^{-1}$, representative of the observed proper motion of BHs in X-ray binaries (Atri et al., 2019). The M70 model is based on the observation of only 16 BHs. We therefore tested two additional alternative models to lower the natal kick magnitudes of pulsars and account for the higher mass of BHs. Once we sample a kick magnitude from the M265 model, we may choose to lower it for the amount of mass falling back to the remnant (Mfb model, implemented as in Fryer et al., 2012) or to down-scale it and normalize it with respect to the remnant mass, as a consequence of linear momentum conservation (G20 model, implemented as in Giacobbo and Mapelli, 2020).

Additionally, we explored two possible common envelope efficiencies ($\alpha_{\rm CE} = 1, 3$) and four metallicities $Z = 0.02$, 0.014, 0.0014, 0.00014: the $\alpha_{\rm CE}$ parameter determines the fraction of orbital energy extracted to eject the common envelope while the Z parameter affects the amount

Table 1: Summary of the twelve combinations of CCSN and natal-kick models simulated for each pair $(Z, \alpha_{\rm CE})$ of metallicity Z and common envelope efficiency $\alpha_{\rm CE}$. The rapid (resp. delayed) CCSN model is based on Fryer et al. (2012) and assumes that the explosion is revived in less than 250 ms (resp. more than 250 ms) after the core bounce; the compactness-based model follows Mapelli et al. (2020). Natal-kick magnitudes are drawn from Maxwellian distributions with root-mean-square speeds σ representative of observed Galactic pulsar proper motions (M265; Hobbs et al., 2005) or BH proper motions (M70; Atri et al., 2019). The Mfb (resp. G20) model lowers the pulsar natal kicks if the remnant is a BH, accounting for fallback (linear momentum conservation) as in Fryer et al. (2012), resp. Giacobbo and Mapelli (2020).

Model	CCSN model	Natal-kick model
dM265	Delayed (>250 ms)	Maxwellian + $\sigma = 265\,{\rm km\,s^{-1}}$
rM265	Rapid (<250 ms)	Maxwellian + $\sigma = 265\,{\rm km\,s^{-1}}$
cM265	Compactness-based	Maxwellian + $\sigma = 265\,{\rm km\,s^{-1}}$
dM70	Delayed (>250 ms)	Maxwellian + $\sigma = 70\,{\rm km\,s^{-1}}$
...	...	...
dMfb	Delayed (>250 ms)	Maxwellian + $\sigma = 265\,{\rm km\,s^{-1}}$ + fallback
...	...	...
dG20	Delayed (>250 ms)	Maxwellian + $\sigma = 265\,{\rm km\,s^{-1}}$ + momentum
...	...	...

of mass lost by the star and its radial expansion, thus, impacts mass transfer processes. For each pair of common envelope efficiency and metallicity explored, there were twelve combinations of CCSN and natal-kick models, for a total of 96 simulated sets, as summarized in Table 1.

3. WR–COs: a Key Progenitor Configuration

In each simulated set, we found that more than about 82% of BCOs had a progenitor in the WR–CO configuration. Most binary neutron stars (BNSs, $\gtrsim 99\%$), black hole–neutron star systems (BHNSs, $\gtrsim 93\%$), and binary black holes (BBHs, $\gtrsim 79\%$) evolved as Wolf–Rayet stars with a black hole (WR–BH) or a neutron star (WR–NS) companion (Fig. 1).

Only approximately 1%–5% of the initial binary population evolved as WR–COs, and few of these WR–COs ended their life as BCOs. At sub-solar metallicity ($Z = 0.0014$, 0.00014) approximately 30% of WR–COs were BCO progenitors; at solar metallicity ($Z = 0.02$, 0.014) only about 5%. The higher production efficiency of BCOs at sub-solar metallicity is determined by the lower mass-loss rates of stellar winds, that determine a higher abundance of BBHs. At these metallicities, stellar winds are quenched (e.g., Vink et al., 2011): stars retain more mass, form heavier compact objects (for instance, a BH in place of a NS), and can shorten the time required to merge via gravitational wave emission (Peters, 1964). We found that BBH production is more sensitive to metallicity and stellar winds than to WR–BH production. In our simu-

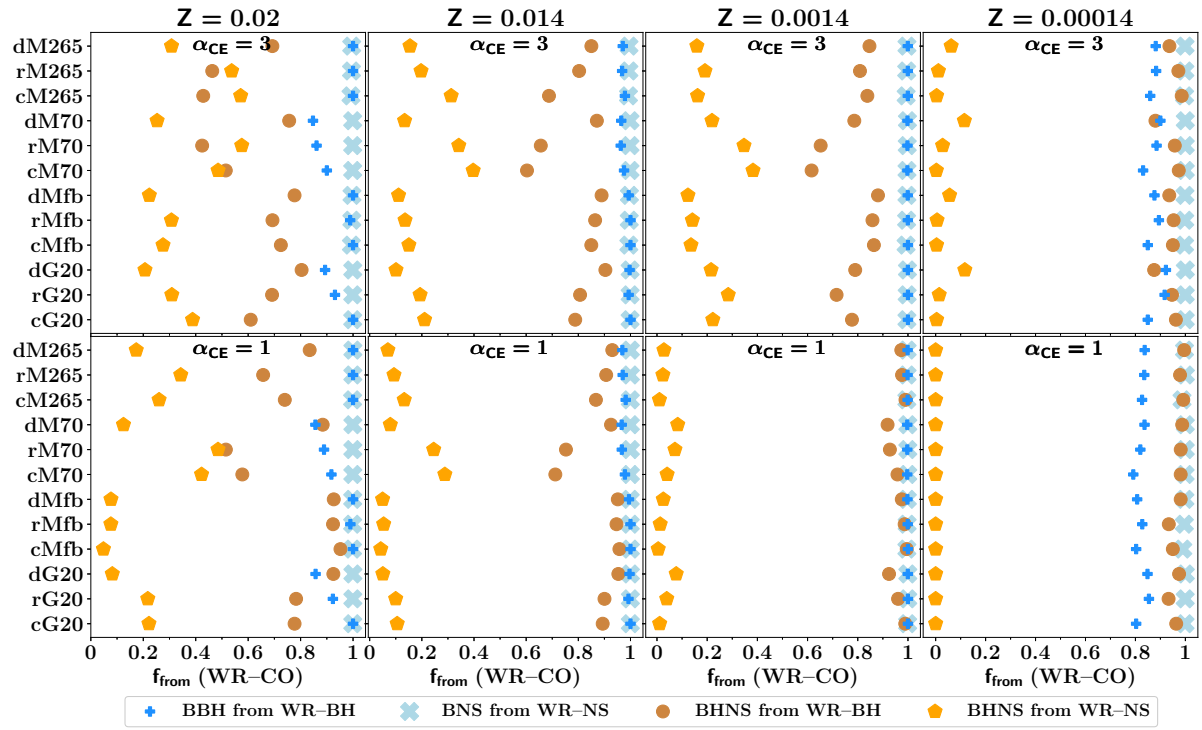

Figure 1: For all the metallicities (columns), $\alpha_{\rm CE}$ efficiencies (rows) and combinations of CCSN and natal-kick models tested in this work (horizontal entries, see Table 1) we show the fraction $f_{\rm from}$ of BCOs with WR–CO progenitors. We distinguish WR–NSs and WR–BHs as possible progenitors of BBHs, BNSs and BHNSs.

lations, WR–BHs always constituted a large fraction of WR–COs, composing approximately 50% of WR–COs at solar metallicity, and approximately 80% at sub-solar metallicity. In contrast, BBHs were the dominant BCO configuration at sub-solar metallicity (about 60%–80%) but they were a rarer BCO type at solar metallicity (less than about 10%).

Assuming different CCSN and natal-kick models had a negligible impact on the fraction $f_{\rm from}$ of BCOs with intermediate WR–CO configurations, inducing variations in $f_{\rm from}$ of less than about 1%. At $Z = 0.02$, 0.014, 0.00014, we observed a larger variability in the fraction $f_{\rm from}$ of BBHs produced by WR–BHs, as shown in Fig. 1. Considering the distribution of $f_{\rm from}$ across CCSN and natal-kick models, for each fixed pair of $(Z, \alpha_{\rm CE})$, we found that nearly every ($\gtrsim 99\%$) BCO at $Z \geq 0.0014$ had a WR–CO progenitor. At $Z = 0.00014$, only about 83%–95% of BCOs evolved as WR–CO (68% credible intervals, Fig. 2). At this metallicity, most BCOs were BBHs and up to 21% of BBHs did not evolve as WR–BH.

We found that the WR–CO configuration, when it is present, always constitutes the last evolutionary stage before BCO formation. WR–COs that are BCO progenitors are produced after one or more mass transfer events, either stable Roche lobe overflows (RLOs) or common envelopes (CEs). Generally, WR–NSs need one or more CE episodes, while WR–BHs prefer RLOs (Fig. 3). Binary stripping enhances the production of WRs, especially if the orbit is tight (semi-major axis $a \lesssim 10^2\,R_\odot$) and the transfer of mass occurs via CE events: RLOs have

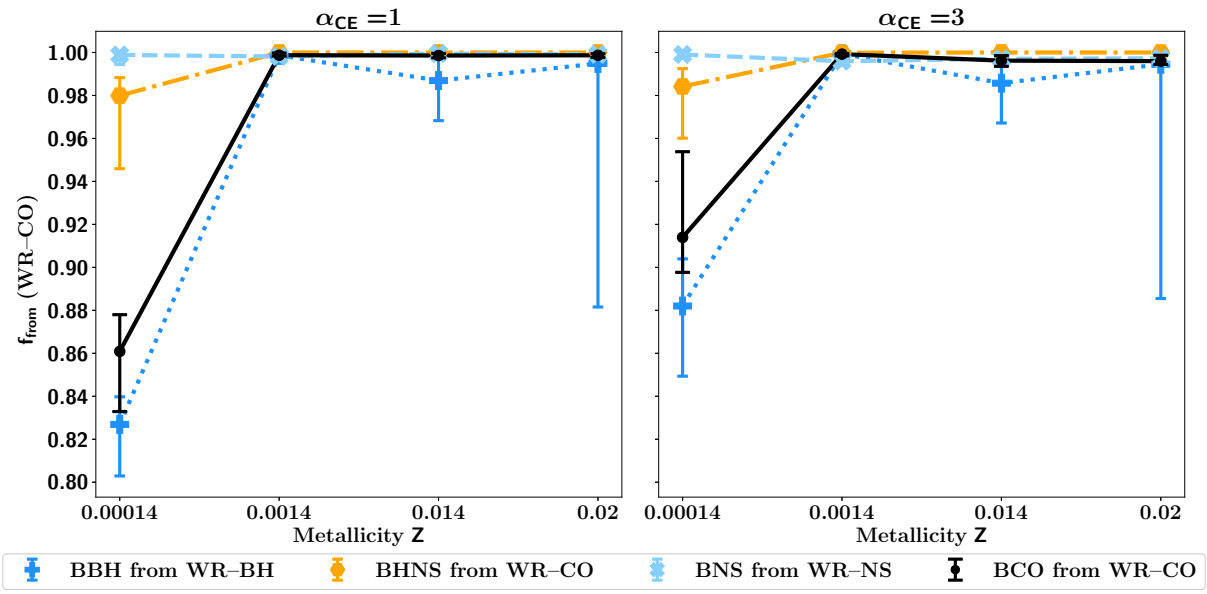

Figure 2: For each pair of (Z, α_{CE}) values, we consider the distribution of the fractions f_{from} of BCOs with WR–CO progenitors across the twelve combinations of CCSN and natal-kick models explored in this work, showing the correspondent median values (scatter points) and 68% credible intervals (error bars). We distinguish BBHs evolved as WR–BHs (dark blue dotted lines, plus sign markers), BNSs evolved as WR–NSs (light blue dashed lines, cross sign markers), BHNSs evolved as either WR–NSs or WR–BHs (orange dash-dotted lines, hexagon markers). We also show the fractions of all BCOs with a WR–CO progenitor (black solid lines, round markers).

longer timescales and are less efficient than CEs (e.g., Marchant et al., 2021). Thus, the WR–BH configuration is more likely to be avoided if the WR progenitor experiences incomplete mass transfer. Wide orbits (with $a \gtrsim 10^2 R_\odot$) or mass transfer episodes initiated in the late stages of core-He burning can prevent the complete stripping of the external hydrogen layers. At $Z = 0.02, 0.014, 0.00014$ the "missing" WR–BH progenitors of BBHs were systems where the companion star was almost a WR, with a residual hydrogen envelope that could constitute approximately 2%–50% of the stellar mass.

Low common envelope efficiencies ($\alpha_{CE} = 1$) limit WR–NSs production: more orbital energy needs to be extracted to expel the CE and the two objects might collide and prematurely merge (Webbink, 1984). At sub-solar metallicity, the weaker stellar winds suppress NS production and WR–NS systems can form only through CE episodes, with additional CEs that are required to produce BNSs or BHNSs. For instance, at $Z = 0.00014$ and for $\alpha_{CE} = 1$ we found that BHNSs with WR–CO progenitors evolve only as WR–BH configuration, with the complete suppression of the WR–NS channel.

We highlight that, in this work, mass transfer is necessary to produce WRs at sub-solar metallicity because we assume that WR stars are stripped pure-helium stars: nearly all of their

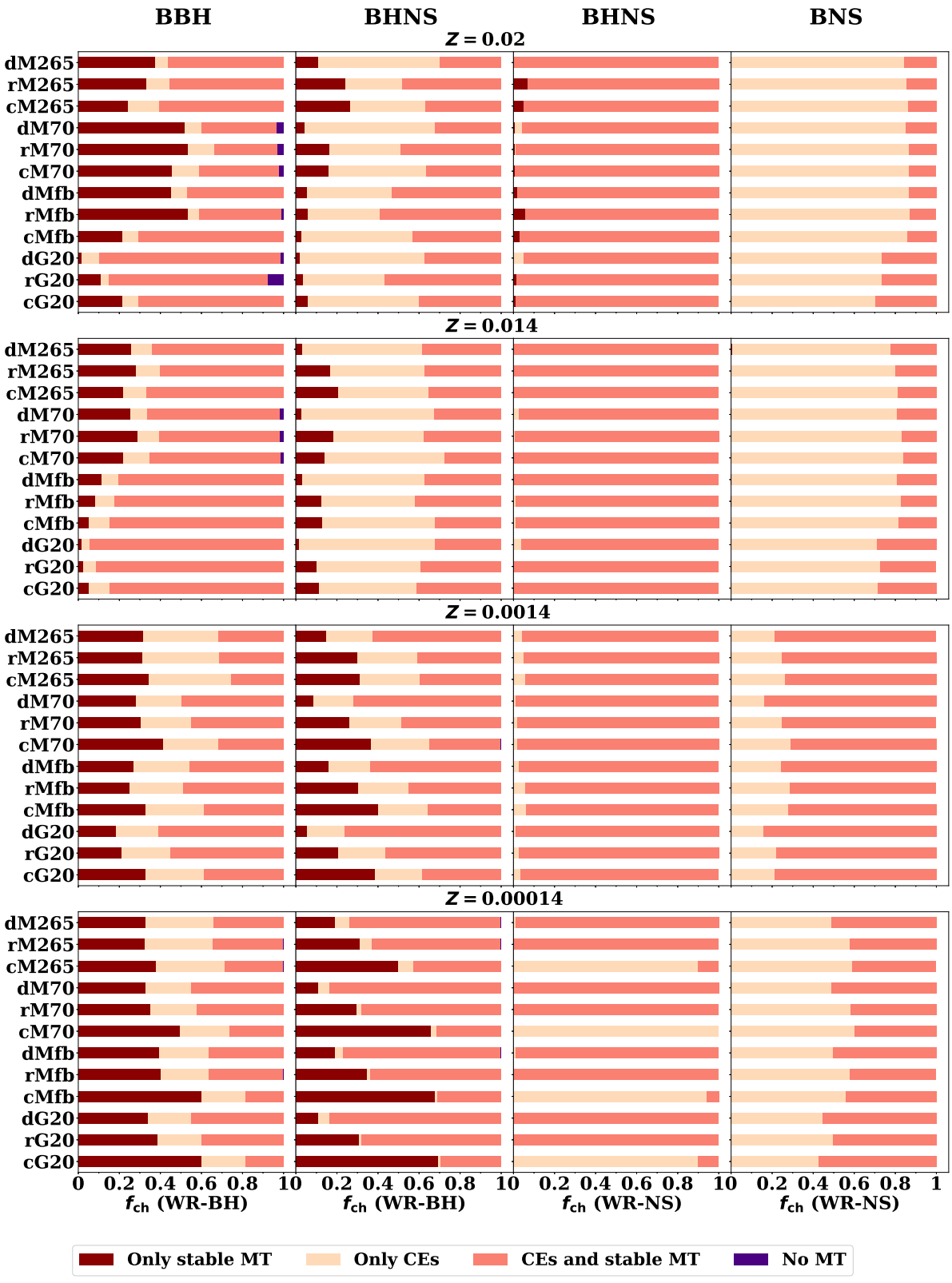

Figure 3: Fractions of BCOs with WR–CO progenitors that evolved with one or more stable mass transfer or CE episode prior to the formation of the WR–CO stage. Here, we show fractions for the sets with $\alpha_{\rm CE} = 3$, different metallicities (rows), and combinations of CCSN and natal-kick models (coloured bars, see Table 1).

mass has to be made of helium ($M_{\rm He} \geq 97.9\,M_{\rm star}$). As pointed out by Shenar et al. (2020), WR stars are defined from a spectroscopical point of view. Theoretical studies should thus be taken with caution and acknowledge that there is a non-trivial but strong dependence between WR formation channels, metallicity, and WR definition. Detailed modelling of stellar spectra is beyond the scope of this work, so here we assumed only a mass threshold to consider a star as a WR, following the spectral models for the WN sub-type stars obtained with the `PoWR` code (Hainich et al., 2014).

4. Cyg X-3: a Probable BCO Progenitor

We compared the orbital properties of WR–COs in our simulations with those of Cyg X-3, the only WR–CO known in the Milky Way (Koljonen and Maccarone, 2017; Esposito et al., 2015). Here we considered a WR–CO system to be a Cyg X-3 candidate if its orbital properties fulfil the following conditions: its orbital period $P_{\rm orb}$ is between 4.5 and 5.1 hours, the WR's mass $M_{\rm WR}$ is between 8 and 14 $M_\odot$, and the CO's mass $M_{\rm rem}$ is lower than 10 $M_\odot$ (Singh et al., 2002; Koljonen and Maccarone, 2017). The BH or NS nature of the CO in Cyg X-3 remains unclear (Zdziarski et al., 2013). Here, we followed the fiducial threshold adopted in Iorio et al. (2023) and assumed that the CO is a BH if its mass is greater than 3 $M_\odot$.

We investigated both solar metallicity values ($Z = 0.02$, 0.014) and found that Cyg X-3 is not a common WR–CO configuration: only about 0.1%–0.01% of the simulated WR–CO population exhibits its properties. However, Cyg X-3 is one of the tightest WR–COs in our simulations, with a semi-major axis of only 3–4 $R_\odot$ (Fig. 4). Since the time required to merge via gravitational-wave (GW) emission reduces in close orbits ($t_{\rm GW} \propto a^4$; Peters, 1964), a WR–CO system with the orbital properties of Cyg X-3 is favoured to be a BCO progenitor. In the most optimistic cases (compactness-based CCSN model, low natal-kicks, as in the G20 or M70 models), up to 80% of Cyg X-3–like binaries are BCO progenitors. Different assumptions on the CCSN and natal-kick models significantly modify the production of NSs, reducing the fraction of Cyg X-3–like binaries that become BCOs to 20% or less. Cyg X-3 candidates hosting a BH have higher chances (approximately 70%–100%) to become BCOs, in agreement with Belczynski et al. (2013). Only less than about 60% of our Cyg X-3–like systems become BCOs through the WR–NS configuration, because most of them break during the second CCSN event. According to these simulations, Cyg X-3–like binaries exhibit properties and evolutionary pathways (e.g., type and mass transfer efficiency, final configurations) that are representative of the WR–CO sub-population that produces BCOs.

5. Summary

In this work, we characterized Wolf–Rayet/compact object binaries (WR–COs) as possible progenitors of binary compact object mergers (BCOs). We accounted for the uncertainties in the theoretical models using a population synthesis approach, evolving the same initial binary population under 96 different combinations of metallicity, CE efficiency, CCSN, and natal-kick models.

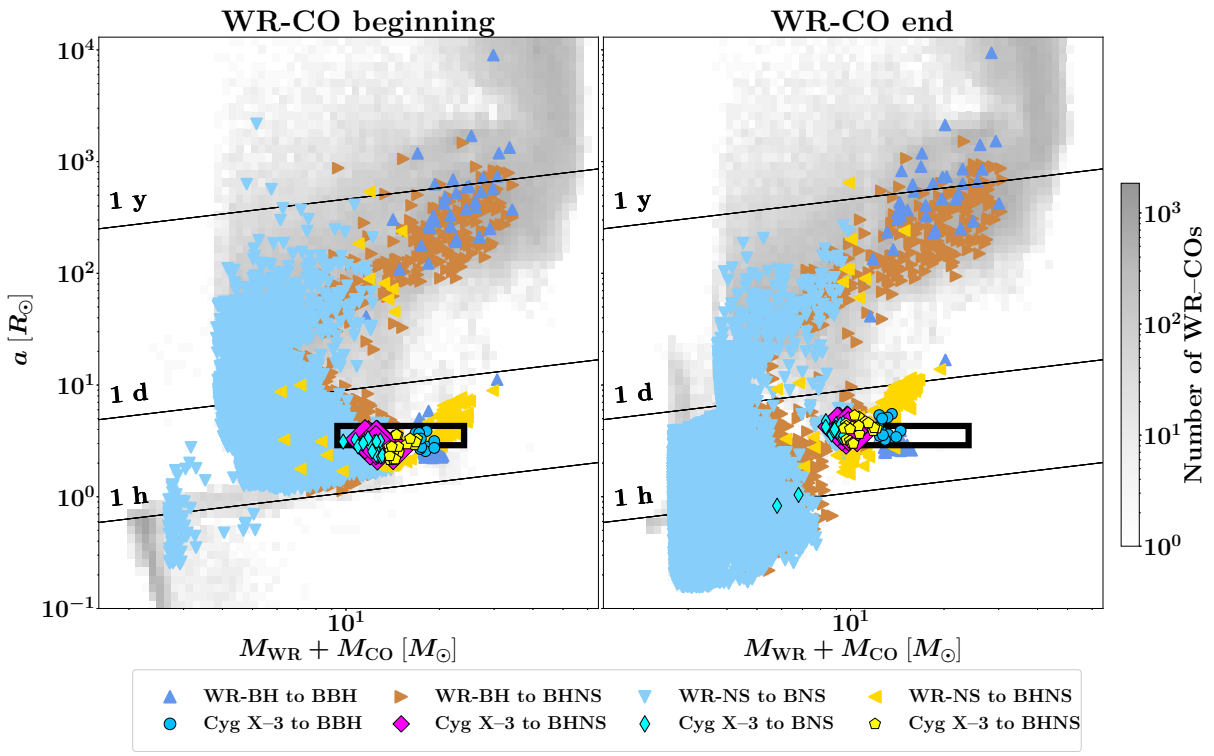

Figure 4: Orbital properties of WR–COs and Cyg X-3 candidates that are BCO progenitors (coloured markers) or have other fates (gray histograms). We show properties at the beginning (*left*) and at the end (*right*) of the WR–CO phase. We show the set evolved with the $\alpha_{\rm CE} = 3$, $Z = 0.02$, delayed CCSN model (Fryer et al., 2012) and the natal-kick model from Giacobbo and Mapelli (2020). The black rectangular box delimits the region of orbital parameters that we use to select Cyg X-3 candidates. Black diagonal lines indicate orbital periods of 1 hour, 1 day and 1 year.

We found that WR–COs are the progenitors of most ($\gtrsim 83\%$) of the simulated BCOs. Mass transfer influences the fraction of BCOs that evolve as WR–COs: incomplete binary stripping prevents the formation of WRs, especially at $Z = 0.00014$. Metallicity affects stellar wind strength and determines the importance of binary stripping in the production of WRs. Natal kicks and CCSN models introduce variability in the remnant masses and orbital separation, and thus in the ability of WR–COs to merge via GW emission within a Hubble time.

Despite their key role as BCO progenitors, only a small fraction of WR–COs (approximately 5%–30%, depending on the metallicity) ends its life as a BCO. Cyg X-3, the only WR–CO candidate in the Milky Way known to date, is one of the tightest ($a \approx 3$–$4\,R_\odot$) WR–COs that we produced. The small orbital separation increases the fraction of Cyg X-3 candidates that could be BCO progenitors. We found that Cyg X-3 has higher chances (approximately 70%–100%) to become a BCO if it is a WR–BH system rather than a WR–NS one: less than 60% of Cyg X-3–like binaries in WR–NS configurations end up as BCOs (or even less than 40%, depending on the assumptions), in agreement with Belczynski et al. (2013).

Acknowledgments

EK acknowledges support from the PRIN grant METE under contract No. 2020KB33TP. Numerical calculations have been made possible through a CINECA-INFN (TEONGRAV) agreement, providing access to resources on Leonardo at CINECA.

Further Information

Author's ORCID identifier

0009-0007-5949-9757 (Erika KORB)

Conflicts of interest

The author declares no conflict of interest.

References

Abbott, R., Abbott, T. D., Acernese, F., Ackley, K., Adams, C., Adhikari, N., Adhikari, R. X., Adya, V. B., Affeldt, C., Agarwal, D., and *1648 more* (LIGO Scientific Collaboration, Virgo Collaboration, and KAGRA Collaboration) (2023) GWTC-3: Compact binary coalescences observed by LIGO and Virgo during the second part of the third observing run. *PhRvX*, **13**(4), 041039. https://doi.org/10.1103/PhysRevX.13.041039.

Atri, P., Miller-Jones, J. C. A., Bahramian, A., Plotkin, R. M., Jonker, P. G., Nelemans, G., Maccarone, T. J., Sivakoff, G. R., Deller, A. T., Chaty, S., Torres, M. A. P., Horiuchi, S., McCallum, J., Natusch, T., Phillips, C. J., Stevens, J., and Weston, S. (2019) Potential kick velocity distribution of black hole X-ray binaries and implications for natal kicks. *MNRAS*, **489**(3), 3116–3134. https://doi.org/10.1093/mnras/stz2335.

Belczynski, K., Bulik, T., Mandel, I., Sathyaprakash, B. S., Zdziarski, A. A., and Mikołajewska, J. (2013) Cyg X-3: A Galactic double black hole or black-hole–neutron-star progenitor. *ApJ*, **764**(1), 96. https://doi.org/10.1088/0004-637X/764/1/96.

Bethe, H. A. and Brown, G. E. (1998) Evolution of binary compact objects that merge. *ApJ*, **506**(2), 780–789. https://doi.org/10.1086/306265.

Bulik, T., Belczynski, K., and Prestwich, A. (2011) IC10 X-1/NGC300 X-1: The very immediate progenitors of BH–BH binaries. *ApJ*, **730**(2), 140. https://doi.org/10.1088/0004-637X/730/2/140.

Crowther, P. A. (2007) Physical properties of Wolf–Rayet stars. *ARA&A*, **45**, 177–219. https://doi.org/10.1146/annurev.astro.45.051806.110615.

Esposito, P., Israel, G. L., Milisavljevic, D., Mapelli, M., Zampieri, L., Sidoli, L., Fabbiano, G., and Rodríguez Castillo, G. A. (2015) Periodic signals from the Circinus region: two new cataclysmic variables and the ultraluminous X-ray source candidate GC X-1. *MNRAS*, **452**(2), 1112–1127. https://doi.org/10.1093/mnras/stv1379.

Fryer, C. L., Belczynski, K., Wiktorowicz, G., Dominik, M., Kalogera, V., and Holz, D. E. (2012) Compact remnant mass function: Dependence on the explosion mechanism and metallicity. *ApJ*, **749**(1), 91. https://doi.org/10.1088/0004-637X/749/1/91.

Giacobbo, N. and Mapelli, M. (2020) Revising natal kick prescriptions in population synthesis simulations. *ApJ*, **891**(2), 141. https://doi.org/10.3847/1538-4357/ab7335.

Hainich, R., Rühling, U., Todt, H., Oskinova, L. M., Liermann, A., Gräfener, G., Foellmi, C., Schnurr, O., and Hamann, W.-R. (2014) The Wolf–Rayet stars in the Large Magellanic Cloud: A comprehensive analysis of the WN class. *A&A*, **565**, A27. https://doi.org/10.1051/0004-6361/201322696.

Hobbs, G., Lorimer, D. R., Lyne, A. G., and Kramer, M. (2005) A statistical study of 233 pulsar proper motions. *MNRAS*, **360**(3), 974–992. https://doi.org/10.1111/j.1365-2966.2005.09087.x.

Iorio, G., Mapelli, M., Costa, G., Spera, M., Escobar, G. J., Sgalletta, C., Trani, A. A., Korb, E., Santoliquido, F., Dall'Amico, M., Gaspari, N., and Bressan, A. (2023) Compact object mergers: exploring uncertainties from stellar and binary evolution with SEVN. *MNRAS*, **524**(1), 426–470. https://doi.org/10.1093/mnras/stad1630.

Koljonen, K. I. I. and Maccarone, T. J. (2017) Gemini/GNIRS infrared spectroscopy of the Wolf–Rayet stellar wind in Cygnus X-3. *MNRAS*, **472**(2), 2181–2195. https://doi.org/10.1093/mnras/stx2106.

Kroupa, P. (2001) On the variation of the initial mass function. *MNRAS*, **322**(2), 231–246. https://doi.org/10.1046/j.1365-8711.2001.04022.x.

Kruckow, M. U., Tauris, T. M., Langer, N., Kramer, M., and Izzard, R. G. (2018) Progenitors of gravitational wave mergers: binary evolution with the stellar grid-based code COMBINE. *MNRAS*, **481**(2), 1908–1949. https://doi.org/10.1093/mnras/sty2190.

Mandel, I. and Broekgaarden, F. S. (2022) Rates of compact object coalescences. *LRR*, **25**, 1. https://doi.org/10.1007/s41114-021-00034-3.

Mapelli, M. (2021) Formation channels of single and binary stellar-mass black holes. In *Handbook of Gravitational Wave Astronomy*, edited by Cosimo Bambi, K. D. K., Stavros Katsanevas, pages 1–65. Springer, Singapore. https://doi.org/10.1007/978-981-15-4702-7_16-1.

Mapelli, M., Spera, M., Montanari, E., Limongi, M., Chieffi, A., Giacobbo, N., Bressan, A., and Bouffanais, Y. (2020) Impact of the rotation and compactness of progenitors on the mass of black holes. *ApJ*, **888**(2), 76. https://doi.org/10.3847/1538-4357/ab584d.

Marchant, P., Pappas, K. M. W., Gallegos-Garcia, M., Berry, C. P. L., Taam, R. E., Kalogera, V., and Podsiadlowski, Ph. (2021) The role of mass transfer and common envelope evolution in the formation of merging binary black holes. *A&A*, **650**, A107. https://doi.org/10.1051/0004-6361/202039992.

Moe, M. and Di Stefano, R. (2017) Mind your Ps and Qs: The interrelation between period (P) and mass-ratio (Q) distributions of binary stars. *ApJS*, **230**, 15. https://doi.org/10.3847/1538-4365/aa6fb6.

O'Connor, E. and Ott, C. D. (2011) Black hole formation in failing core-collapse supernovae. *ApJ*, **730**(2), 70. https://doi.org/10.1088/0004-637X/730/2/70.

Peters, P. C. (1964) Gravitational radiation and the motion of two point masses. *PhRev*, **136**(4B), B1224–B1232. https://doi.org/10.1103/PhysRev.136.B1224.

Sana, H., de Mink, S. E., de Koter, A., Langer, N., Evans, C. J., Gieles, M., Gosset, E., Izzard, R. G., Le Bouquin, J.-B., and Schneider, F. R. N. (2012) Binary interaction dominates the evolution of massive stars. *Sci*, **337**, 444–446. https://doi.org/10.1126/science.1223344.

Schneider, F. R. N., Podsiadlowski, Ph., and Laplace, E. (2023) Bimodal black hole mass distribution and chirp masses of binary black hole mergers. *ApJL*, **950**(2), L9. https://doi.org/10.3847/2041-8213/acd77a.

Shenar, T., Gilkis, A., Vink, J. S., Sana, H., and Sander, A. A. C. (2020) Why binary interaction does not necessarily dominate the formation of Wolf–Rayet stars at low metallicity. *A&A*, **634**, A79. https://doi.org/10.1051/0004-6361/201936948.

Singh, N. S., Naik, S., Paul, B., Agrawal, P. C., Rao, A. R., and Singh, K. Y. (2002) New measurements of orbital period change in Cygnus X-3. *A&A*, **392**(1), 161–167. https://doi.org/10.1051/0004-6361:20020923.

Tauris, T. M., Kramer, M., Freire, P. C. C., Wex, N., Janka, H.-T., Langer, N., Podsiadlowski, Ph., Bozzo, E., Chaty, S., Kruckow, M. U., Heuvel, E. P. J. v. d., Antoniadis, J., Breton, R. P., and Champion, D. J. (2017) Formation of double neutron star systems. *ApJ*, **846**(2), 170. https://doi.org/10.3847/1538-4357/aa7e89.

Vink, J. S., Muijres, L. E., Anthonisse, B., de Koter, A., Gräfener, G., and Langer, N. (2011) Wind modelling of very massive stars up to 300 solar masses. *A&A*, **531**, A132. https://doi.org/10.1051/0004-6361/201116614.

Webbink, R. F. (1984) Double white dwarfs as progenitors of R Coronae Borealis stars and Type I supernovae. *ApJ*, **277**, 355–360. https://doi.org/10.1086/161701.

Zdziarski, A. A., Mikołajewska, J., and Belczyński, K. (2013) Cyg X-3: a low-mass black hole or a neutron star. *MNRAS*, **429**(1), L104–L108. https://doi.org/10.1093/mnrasl/sls035.